8.3 OBJECT KINETIC MONTE CARLO SIMULATIONS OF RADIATION DAMAGE ACCUMULATION IN TUNGSTEN—

G. Nandipati, W. Setyawan, K. J. Roche, R. J. Kurtz (Pacific Northwest National Laboratory) and B. D. Wirth (University of Tennessee)

OBJECTIVE

The objective of this work is to understand the accumulation of radiation damage created by primary knock-on atoms (PKAs) of various energies, at 300 K and for a dose rate of 10^{-4} dpa/s in bulk tungsten using the object kinetic Monte Carlo (OKMC) method.

SUMMARY

We used the lattice-based object kinetic Monte Carlo code; *KSOME* [1] to perform simulations of radiation damage accumulation in bulk tungsten at 300 K and for a dose rate of 10^{-4} dpa/s, up to a dose of 1.0 dpa. These are ad-hoc irradiation simulations performed using a set of cascades with the same PKA energies. In this study, eight different irradiation simulations were performed using eight sets of cascades with PKA energies of 10, 20, 30, 40, 50, 60, 75 and 100 keV. Both the number density of vacancies and vacancy clusters in the simulation box appears to saturate with increasing dose in the simulation using cascades with PKA energies of 40, 50, 60, 75, 100 keV, while the same parameters increase linearly with dose in the simulations using cascades with PKA energies of 10, 20 and 30 keV. In all simulations the average vacancy cluster size remained constant with dose. However, the vacancy cluster size increases with cascade PKA energy.

PROGRESS AND STATUS

Simulation Details

Simulations were performed using a non-cubic box with dimensions 95.10 x 96.37 x 97.00 nm^3 (300a x 304a x 306a, where *a* is the lattice constant of tungsten), with each axis parallel to a <100> type direction. Each defect is allowed to hop to one of eight possible body-centered cubic nearest neighbor lattice sites at a distance of *a*/2 <111>, Finite periodic boundary conditions were adopted in all three directions i.e. periodic boundary conditions are applied but whenever a mobile object moved a distance larger than the average grain size, it is removed from the simulation, and it is no longer tracked. In the present simulations, we used an average grain size of 2 μm and no intragranular traps were considered.

The values of the binding energies of defects used in the present annealing simulations were taken from the *ab initio* calculations of Becquart *et al*. [3] while the migration barriers were taken from MD simulations [4] using an EAM potential for W [5]. In the present simulations, SIA clusters larger than size five were constrained to diffuse in 1D along one of four <111> directions. SIA clusters up to size five were allowed to change their direction of 1D motion via rotation and thereby perform a mixed 1D/3D motion. The activation barrier for changing direction from one <111> direction to another is 0.38 eV [6]. The direction of 1D motion was assigned randomly to the SIAs at the start of a simulation, and interstitial clusters of all sizes are assumed to be glissile (mobile). Their migration/diffusion rates decrease with increasing cluster size (n) according to $\nu_o n^{-1.0}$ (ν_o = 6 x 10^{12} s^{-1}) while the migration barrier is taken to be independent of cluster size.

For a single vacancy, the activation barrier for diffusion is taken as 1.30 eV [4], and vacancy clusters larger than five are assumed to be immobile. But vacancy clusters of all sizes are allowed to emit mono-vacancies. All mobile vacancy clusters migrate in 3D, and their diffusion rates decrease with cluster size (n) according to $\nu_o(q^{-1})^{n-1}$ (ν_o = 6 x 10^{12} s^{-1}, q = 1000) [3]. The vacancy (SIA) dissociation rate is given by $\Gamma_d = \nu_d \exp((E_m + E_d)/k_B T)$, where E_d is the binding energy of a vacancy (SIA) to a vacancy (SIA) cluster, and E_m is the migration energy of a single vacancy (SIA). We have assumed that defect clusters of all sizes and types are spherical objects, and their capture radii were obtained from Reference [3].

Individual cascades are randomly selected from the database of cascades of a particular PKA energy and inserted into the simulation box at random positions based on the cascade production rate. The

production rate of cascades, which is the number of cascades produced in the simulation cell per second, dose rates and the accumulated dpa (displacements per atom) are calculated based on the NRT displacements per cascade (ν_{NRT}). [7]

Results

Cascades were created using MD simulations as described in Ref. [2] Simulations were performed at 300 K and for the dose rate of 10^{-4} dpa/s. Since no intragranular traps are considered in the present simulation, interstitial clusters, which diffuse very fast, are very quickly either absorbed at grain boundaries or recombine. Therefore, only the data on vacancy type defects are presented in this report.

Figures 1(a-c) shows plots of the density of vacancies and vacancy clusters, and average vacancy cluster sizes as a function of dose for the irradiation simulations performed using cascades of various PKA energies. In the irradiation simulations using 10 keV cascades, both the density of vacancies and vacancy clusters increases linearly from very low doses all the way up to a dose of 1.0 dpa. In case of 20 and 30 keV simulations densities increase linearly with dose above 0.1 dpa. The rate of growth of these

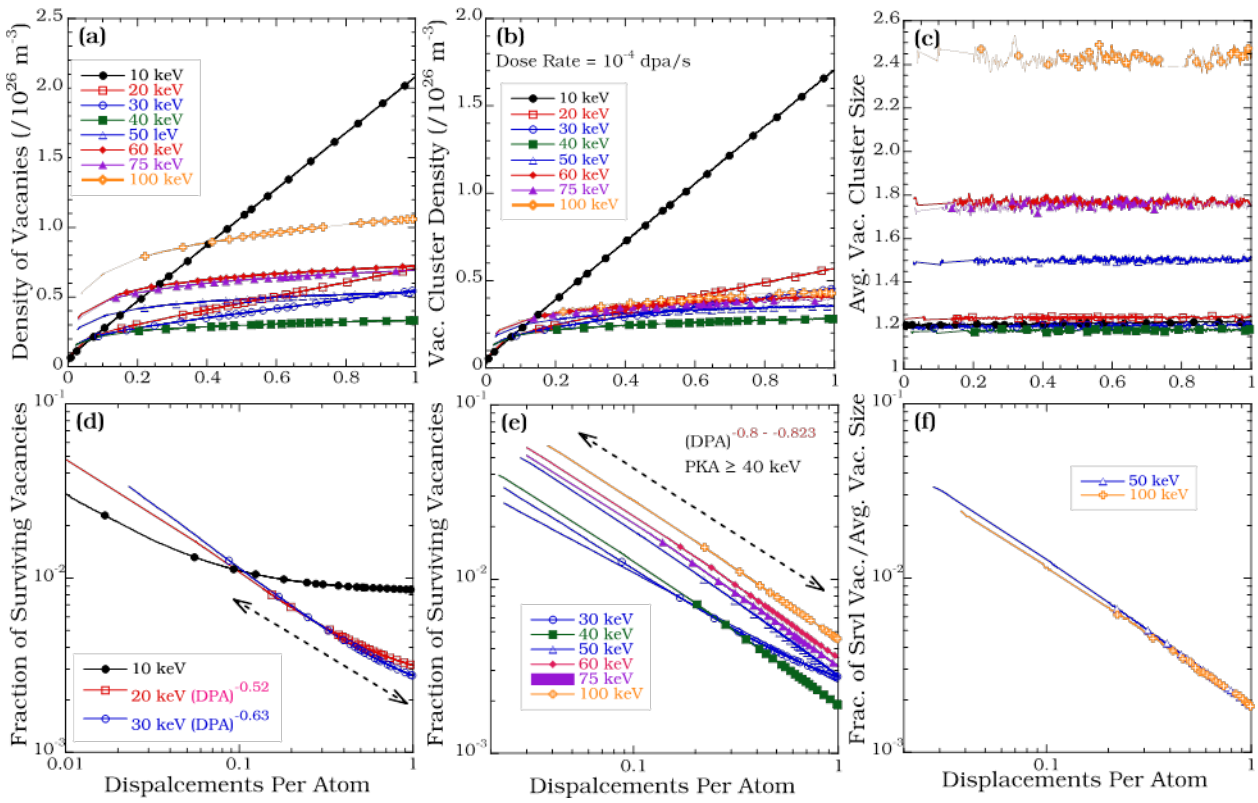

Figure 1. Comparison of damage accumulation in tungsten at 300 K as a function of dose for various PKA energies (a) Vacancy cluster density (b) density of vacancies (c) average vacancy clusters size (unit: number of vacancies), fraction of surviving vacancies (d) 10, 20, 30 keV (e) 40, 50, 60, 75, 100 keV (f) ratio of surviving vacancies and average vacancy cluster size for 50, 100 keV simulations.

parameters with dose decreases with increasing PKA energy (Figures 1(a-b)). While in the case of simulations performed using 30, 40, 50, 60, 75 and 100 keV cascades, the density of both vacancy clusters and vacancies appears to saturate or to closely approach saturation with dose (Figures 1(a-b)). Note that for the same irradiation dose, the retained irradiation damage decreases with PKA energy from 10 to 30 keV, while it increases for PKA energies greater than 30 keV. This behavior suggests that retained damage saturates at a much lower dose in case of a radiation source with higher PKA energies

than in the case of a radiation source with lower PKA energies. More importantly, the shift in the behaviorof retained damage with PKA energy occurs at a PKA energy of 40 keV, which also corresponds to a significant change in the defect cluster size distribution obtained from the MD cascades. In all cases, the average vacancy cluster size remained constant with dose but it increased with cascade PKA energy (Figures 1(c)).

Figures 1(d-e) shows plots of the fraction of surviving vacancies, while Figure 1(f) shows the ratio of the fraction of surviving vacancies and the average vacancy cluster size for 50 and 100 keV PKA simulations. Note that the fraction of surviving vacancies shown in Figures 1(d-e) is the ratio of surviving vacancies over the total number of vacancies from all the cascades inserted to reach a particular dose. In the case of 10 keV, although the fraction of surviving vacancies decreases with dose up to 0.1 dpa, it seems to saturate for higher doses. While the behavior is similar in the case of 20 and 30 keV, it is hard to say if it is saturated or not at the dose of 1.0 dpa. For higher PKA energies the behavior is similar in all PKA energies. The surviving fraction exhibits power-law decay with increasing dose with an exponent in the range 0.8-0.823 (Figure 1(e)). However, the fraction of surviving vacancies for all the PKA energies will collapse into a single curve (Figure 1(f)) when scaled with average vacancy cluster size from Figure 1(c). Note that the surviving fraction of vacancies in the case of 20 and 30 keV also exhibits power-law decay with exponents of 0.52 and 0.63, respectively.

Figures 2 and 3 shows snapshots of the vacancy distributions in the simulation box at a dose of 1.0 dpa for various PKA energies. The color scale in Figures 2 and 3 goes from a minimum of one vacancy to a maximum of 5-vacancies per cluster. From Figures 3 and 4, one can see that the spatial distribution of vacancy clusters is random and based on the average cluster size from Figure 1(c), a significant fraction of vacancy clusters are mono-vacancies. Even though the average cluster size increases with PKA energy, a significant fraction of vacancy clusters are mono-vacancies even at higher PKA energies, and the largest vacancy cluster is of size 5 for the 100 keV simulation. As expected, this behavior is due to lack of mono-vacancy diffusion and dissociation of small vacancy clusters at 300 K. Interestingly, a closer look reveals what looks like the ordering of vacancy clusters, which appear as bands. These bands are more obvious in Figure 2(b), which is the microstructure at 1.0 dpa for the irradiation simulation using 20 keV cascades. However, the bands seen in Figure 2(b) appear and disappear randomly with dose.

Future Work

Further simulations are being carried out to understand defect accumulation at various dose rates, PKA energies, temperatures, simulation cell and grain size.

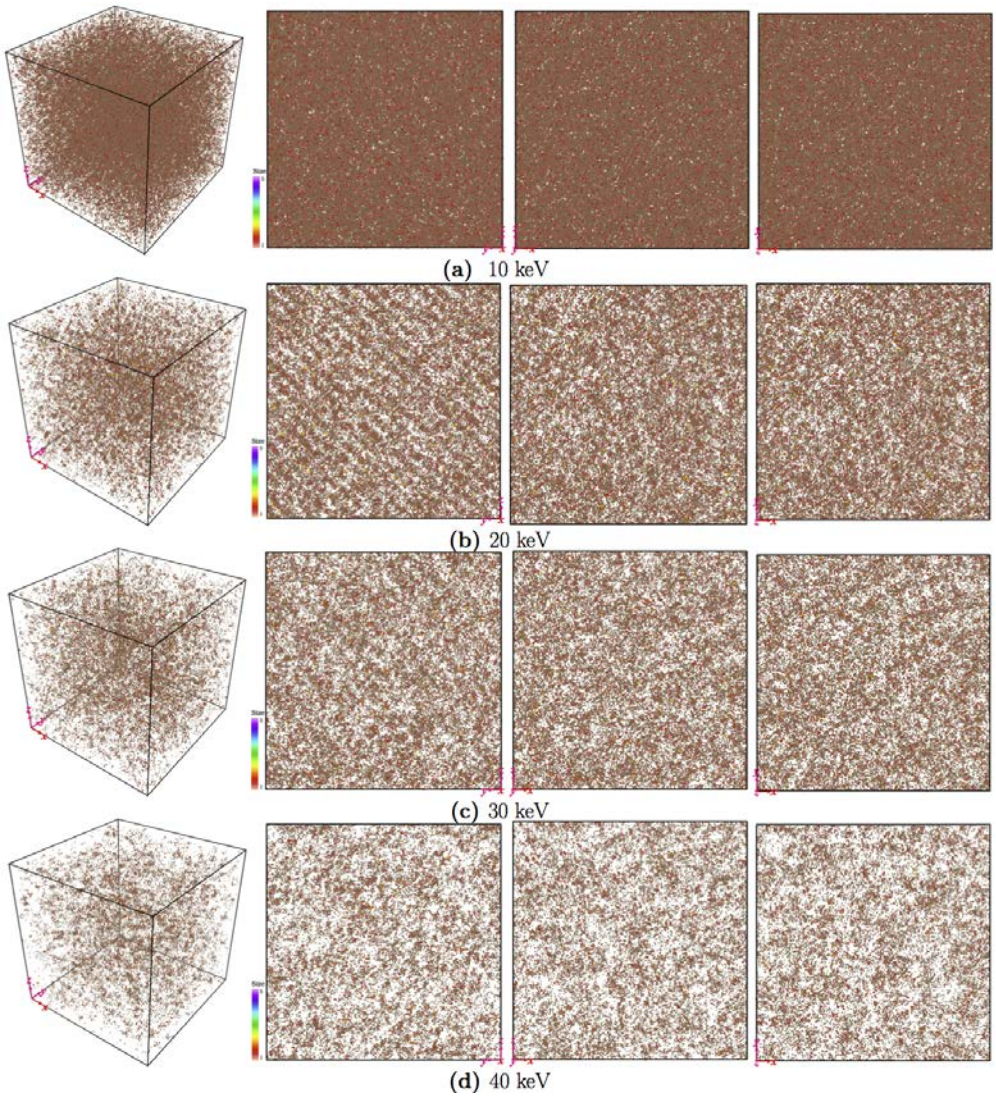

Figure 2. Snap shots of vacancy clusters in the simulation box at 1.0 dpa (a) 10 keV (b) 20 keV (c) 30 keV (d) 40 keV.

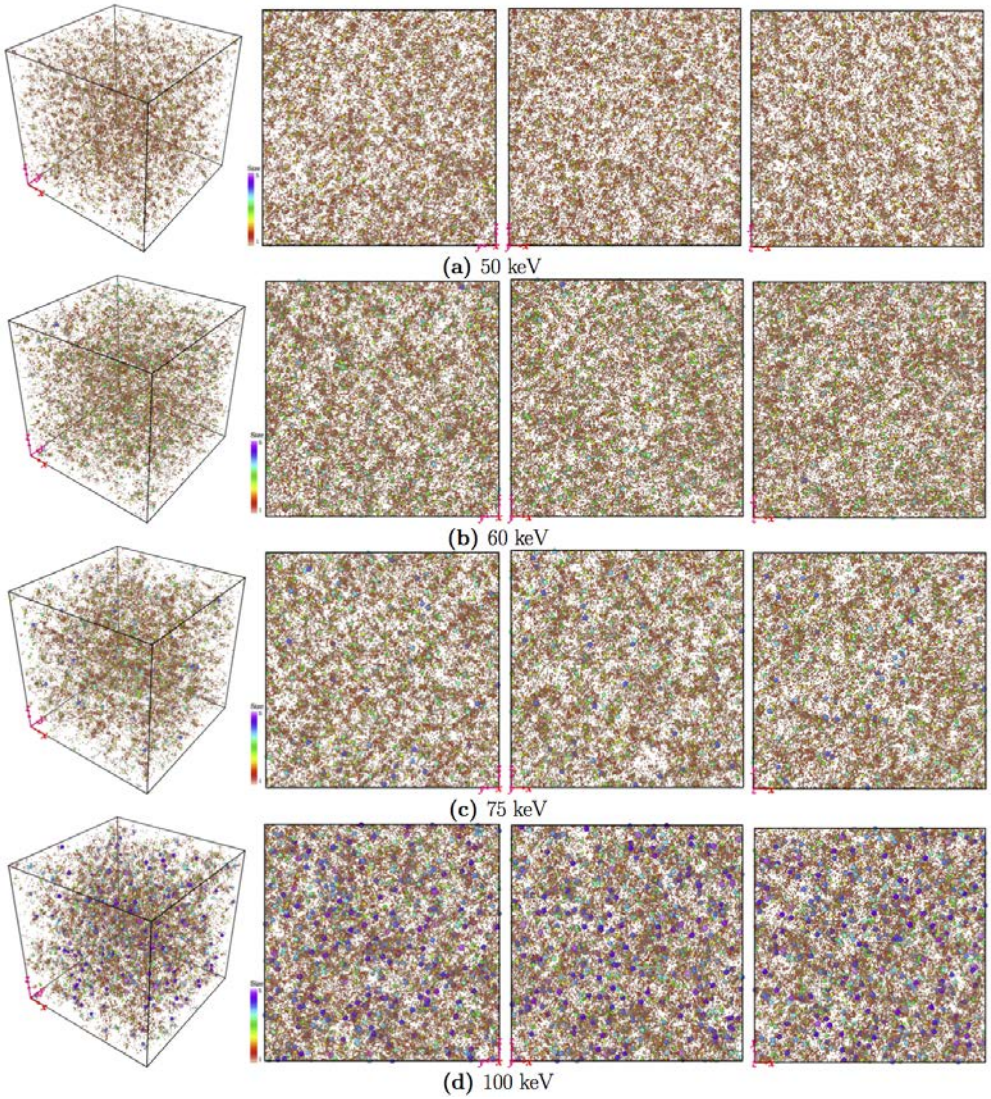

Figure 3. Snap shots of vacancy clusters in the simulation box at 1.0 dpa (a) 50 keV (b) 60 keV (c) 75 keV (d) 100 keV.

Acknowledgement

These simulations were performed on CARVER and HOPPER at National Energy Research Scientific Computing Center (NERSC), Argonne National Lab, MCS Workstations and PNNL's PIC systems.

References

[1] G. Nandipati *et al* Semiannual Progress Report DOE/ER-0313/54, June 2013, 179-183
[2] W. Setyawan *et al* Semiannual Progress Report DOE/ER-0313/54, June 2013, 200-204
[3] C. S. Becquart *et al.* J. Nucl. Mater. 403 (2010) 75
[4] T.Faney, N.Juslin, B.D.Wirth,(*private communication)*.
[5] N.Juslin, B.D.Wirth, J. Nucl. Mater. 432(2013)61.
[6] D. A. Trentyev, L. Malerba, M. Hou, Phys. Rev. B 75 (2007) 104108.
[7] M.J. Norgett, M.T. Robinson, I.M. Torrens, Nucl. Eng. Des. 33 (1975) 50.